Journal of Applied Polymer Science

Polypropylene/polystyrene blends prepared by diffusion and subsequent polymerization in polypropylene pellets after injection molding

Fang Chen, Zhao-Xia Guo, Jian Yu
Key Laboratory of Advanced Materials (MOE), Department of Chemical Engineering, Tsinghua University, Beijing, 100084, People's Republic of China
Correspondence to: Z.-X. Guo (E-mail: guozx@mail.tsinghua.edu.cn) and J. Yu (E-mail: yujian03@mail.tsinghua.edu.cn)

ABSTRACT: PP/PS quasi-nanoblend pellets were synthesized by diffusion and subsequent polymerization of styrene in iPP pellets via a two-step procedure and then processed by injection molding. The PS distributions along the thickness direction of the molded bars were investigated by Micro-FTIR, showing almost homogeneous distribution no matter whether the PS distribution in the blend pellets is homogeneous. The morphology of the molded bars was investigated by FESEM, revealing two types of particles (small spherical and bigger irregular-shaped complex aggregates) and good interfacial adhesion between particles and matrix. The particles are mainly in nano and submicron sizes, and only few particles approach 1 μm. The mechanical properties of the molded bars were evaluated by uniaxial tensile testing, showing a significant reinforcing effect without significantly loosing ductility. The yield strength of all the blends increase 20–27% compared to neat PP and the elongations at break are all over 300%. The remarkable mechanical properties of the molded bars were correlated with their morphology. © 2016 Wiley Periodicals, Inc. J. Appl. Polym. Sci. **2016**, *133*, 43983.

KEYWORDS: blends; mechanical properties; nanostructured polymers; polyolefins; polystyrene

Received 29 February 2016; accepted 25 May 2016
DOI: 10.1002/app.43983

INTRODUCTION

Polymer nanoblends or quasi-nanoblends, in which the size of the dispersed phase is smaller than or approaches 100 nm, have long been an interesting research topic,[1–16] since they are expected to have better properties than the corresponding microblends obtained by conventional methods such as melt mixing or solution casting. Some examples of such blends have shown indeed remarkable mechanical properties.[1,3,6,11,14,15,17–21] For example, the PP/PS nanoblend films reported by Liu *et al.*[3] exhibit an increase of up to 50% in tensile strength and an increase of up to 160% in elongation at break as compared to neat PP film and the PP/PMMA nanoblend films reported by Zhu *et al.*[11] have considerably higher yield stress than neat PP film and maintained good ductility of PP film with up to 28% PMMA, although both PP/PS and PP/PMMA blends prepared by conventional melt mixing are macrophase-separated because of immiscibility of the polymer pairs and not useful in practice. Both types of nanoblends were prepared using supercritical CO_2-assisted infusion and subsequent polymerization of the monomer (St or MMA) in the amorphous regions of PP films, and the improved mechanical properties were attributed to the enhanced interfacial adhesion resulted from the entanglement of PS and PP molecules near the phase boundary.[3] Using *in situ* polymerization and *in situ* compatibilization reactive extrusion process, Hu and Cartier[1] obtained PP/PA6 nanoblends which display a very ductile behavior, in contrast to the brittle behavior of the microblend synthesized without the formation of PP-*g*-PA6 graft copolymer acting as compatibilizer. Using high-shear processing without any additives, Shimizu *et al.*[6] obtained PVDF/PA11 80/20 nanoblend that possesses excellent ductility, 560% higher than the corresponding microblend prepared with classical low-shear processing, although the yield stress is similar for the two types of blends. Using solution blending method, Kausar *et al.*[14] obtained PS-NH_2/aramid (with -COCl as end groups) nanoblends and compared them with uncompatibilized immiscible PS/aramid blends in view of mechanical properties. The nanoblends show much better tensile strength and elongation at break than the microblends, even with only an incorporation of 10% of the aramid both tensile strength and elongation at break approach those of neat aramid.

In a previous paper,[10] our research group reported a method to prepare PP/PS quasi-nanoblend pellets by diffusion and subsequent polymerization of styrene in isotactic polypropylene pellets. Unlike the supercritical CO_2-assisted infusion and subsequent polymerization, the method uses water as the dispersing medium without adding any swelling agent of the

substrate. The driving force for the diffusion of St into the amorphous regions of iPP pellets at a temperature around α relaxation is its better affinity to iPP than to water ascribed to their similarity in polarity. The initiator BPO can diffuse into iPP pellets after diffusion of St through the diffusion path of St. Because the product of polymerization is in the form of pellet, an important advantage of the method is applicability of the product for direct use in plastic production without precompounding. Injection molding is a widely used processing method for plastics, and a variety of PP-based plastic materials are produced by injection molding. In this article, PP/PS quasi-nanoblend pellets are prepared in bigger scales and processed by injection molding, and the mechanical properties of the molded bars are evaluated and correlated with their morphology.

EXPERIMENTAL

Materials

Commercial grade iPP pellets, T03-H, with a density of 0.90 g/cm^3, and diameter of approximately 4 mm, were from SINOPEC, China. Polyvinyl alcohol (PVA) with a degree of polymerization of 1750 ± 50 and a degree of alcoholysis of 88% was purchased from Beijing Organic Chemical Plant. Styrene (St, Fuchen Chemical Reagent Plant, Tianjin) was purified by vacuum distillation. Benzoyl peroxide (BPO) was purified by recrystallization twice from chloroform/methanol. Chloroform and methanol were analytical grade and used as received.

Synthesis of PP/PS Quasi-Nanoblend Pellets

The diffusion and subsequent polymerization of St in iPP pellets were carried out using a previously reported procedure with slight modification.[10] A two-step procedure, in which diffusion and polymerization were carried out in different flasks, was envisaged. Thus, iPP pellets (600 g, unless it is the variable), pure water (525 mL), and aqueous PVA (75 mL, 0.8% in water) were mixed in a 2000 mL flask equipped with a condenser and a mechanical stirrer and heated to 90 °C. St (25 wt % to iPP, unless it is the variable) was added to the mixture. The diffusion of St into iPP pellets was carried out at 90 °C for 3 h. Then, the pellets were separated by vacuum filtration and transferred into another flask containing 600 mL of deionized water preheated to 90 °C. BPO (0.5 wt % to St) was added with the aid of chloroform (0.8 mL per 0.1 g of BPO). After 3 h of polymerization at 90 °C, the pellets were separated by filtration after cooling to room temperature, washed and dried to a constant weight. PS content is defined as the weight ratio of total PS formed by polymerization to the initial iPP pellets. The monomer efficiency is defined as the weight ratio of total PS formed by polymerization to the initial St used for diffusion.

Measurement of Monomer Conversion

Monomer conversion was measured by gravimetric method. It is the weight ratio of PS contained in the blend pellets to St diffused into the pellets. The former was determined by the weight gain of the blend pellets (compared to the original iPP pellets) after thorough drying to remove unreacted St. The latter was determined by the weight gain of the blend pellets (compared to the original iPP pellets) simply scrubbed with filter paper to remove water on the pellet surface without drying in an oven after polymerization for 180 min.

Injection Molding

The synthesized PP/PS blend pellets were used directly for injection molding in an injection molding machine (ZT-630, Zhenda Machinery, Zhejiang, China). During the injection processing, the temperatures of the region I, II, III, and the nozzle were set at 200 °C, 205 °C, 210 °C, and 220 °C, respectively. The injection-molded dumbbell-shaped bars had an overall length of 150 mm, a width in the gauge section of 10 mm, and a thickness of 4 mm.

Microscopic Fourier Transform Infrared Spectroscopy

Films with a thickness of 15 μm were cut through the cross-section of injection-molded bars or through the center of blend pellets by a microtome (YD-1508R, Zhejiang Jinhua Yidi Medical Equipment Factory). Then, Microscopic Fourier Transform Infrared Spectroscopy (Micro-FTIR) was performed on Thermo-Nicolet 6700 FT-IR and Nicolet Continuum FTIR Microscope with a step length of 100 μm. FTIR spectra were recorded along the thickness direction of injection-molded bars or diameter of single pellets. A_1/A_2 is defined as the ratio of the peak areas of the absorptions at 758 cm^{-1} (PS) and 1167 cm^{-1} (iPP), reflecting PS/PP at the measured position.

Measurement of PS Grafting

The percentage of PS grafting is defined as the weight ratio of grafted PS to PP, and measured as follows: PP/PS blend pellets were dissolved in boiling xylene, after slight cooling THF was added to precipitate PP and PP-*g*-PS, and then filtered. The powdery precipitate was stirred in refluxing THF for 8 h to remove any remaining un-grafted PS, then cooled, filtered, and dried. A thin film was prepared by melt-pressing and analyzed by FTIR to get an A_1/A_2 ratio. The process of refluxing in THF was repeated until A_1/A_2 ratio was constant. The percentage of PS grafting was calculated according to a calibration curve obtained from melt-blended films of PS/PP blends of different compositions.

Field Emission Scanning Electron Microscopy

JSM-7401 field emission scanning electron microscope was used to investigate the morphology of the cross-sections of single pellets and injection-molded bars at an accelerating voltage of 1 and 3 kV, respectively. The injection-molded bars were cryo-fractured in liquid nitrogen, while the pellets were cut using the same cutting procedure as for Micro-FTIR and then etched as follows: the cut discs were stirred for 1 h in a mixture of water (5 g), sulfuric acid (6 g, 95%), orthophosphoric acid (9 g, 85%), and potassium permanganate (0.08 g) to remove the amorphous regions of iPP for better observation. The samples were washed in water for 5 min and then in acetone for another 5 min in an ultrasonic cleaner before drying. Particle sizes were counted with the aid of the Smile View software.[10]

Measurements of Mechanical Properties

The tensile properties were measured according to ISO 527 (GB/T 1040.1-2006). The tensile testing was performed on a GT-TCS 2000 machine (Gotech) at a crosshead speed of 50 mm/min. The average of five measurements was reported.

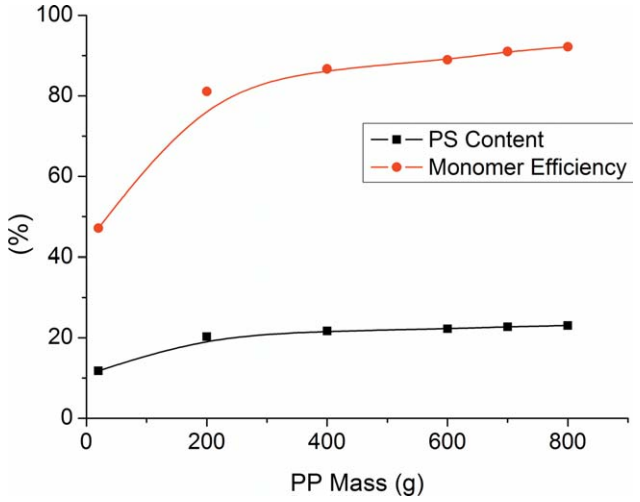

Figure 1. PS contents and monomer efficiencies at different amounts of PP. [Color figure can be viewed in the online issue, which is available at wileyonlinelibrary.com.]

RESULTS AND DISCUSSION

Preparation of PP/PS Quasi-Nanoblend Pellets

PP/PS quasi-nanoblend pellets were prepared in a much bigger scale than that reported previously to produce enough pellets for injection molding. A two-step procedure, where the pellets were separated from the original flask after diffusion of St at 90 °C to remove excess St which is not diffused into the pellets and then transferred into a new flask for initiation and polymerization, was used in order to avoid polymerization-induced diffusion of St during polymerization and thus obtain fine phase morphology. Polymerization conditions were 90 °C and 3 h[10] in order to get a reasonable reaction rate and high monomer conversion because BPO was used as the initiator. To increase the process efficiency, the effects of the amounts of PP and St on PS content and monomer efficiency were investigated.

The amount of PP was varied from 20 to 800 g in keeping the amounts of water and aqueous PVA constant. PP/St/BPO proportion was fixed at 100/25/0.125. As shown in Figure 1, the PS content in the blend pellet is 11% when 20 g of PP pellets is used, and increases to 20% when the amount of PP increases to 600 g, and then almost levels off with increasing amount of PP. Accordingly, the monomer efficiency is low (47%) when the amount of PP is small (20 g), and much higher monomer efficiency (89%) is achieved when much more PP pellets (600 g) are used. Considering that the monomer conversion during polymerization is very high,[10] even for the sample prepared with 20 g PP pellets of Figure 1, the monomer conversion is 91.3%, the monomer efficiency is mainly controlled by the diffusion efficiency of St (i.e., the ratio of the St diffused into the pellets to total St) in the diffusion step. The low monomer efficiency associated with small amount of PP pellets can be attributed to low diffusion efficiency of St.

When St was added to the flask containing water, PVA and iPP pellets at 90 °C with stirring, it was distributed into two parts. Some St was adsorbed on the surfaces of iPP pellets and other St suspended in water as monomer droplets. The distribution ratio of St depends on water/pellet ratio. As diffusion of St into iPP pellets proceeds with time, the St in the monomer droplets migrates through the water to the surfaces of iPP pellets. The migration is more efficient when the two types of species are in direct contact by stirring. When the amount of iPP pellets is small such as 20 g, a considerable amount of St is in the form of droplets because water/pellet ratio is huge, and the migration of St from the monomer droplets to the surfaces of iPP pellets is not efficient because the contacting chance for the two types of St-containing species is small, and therefore a significant amount of St is wasted in water and the monomer diffusion efficiency is low (51.6%). By contrast, when the amount of iPP pellets is large enough such as 600 g, most St is adsorbed on the surfaces of iPP pellets and the migration of St from the monomer droplets to the surfaces of iPP pellets is efficient because of the low water/pellet ratio, resulting in a very high monomer diffusion efficiency (estimated to be around 95%).

Fixing the amount of PP at 600 g and BPO/St ratio at 0.5%, the amount of St was varied from 5% to 23% relative to PP under constant amounts of water and aqueous PVA. As shown in Figure 2, the PS content in the blend pellet increases with increasing amount of St, revealing that the composition of the PP/PS blend pellets can be controlled by St/PP ratio. When the addition of St is small (5% to iPP), the monomer efficiency is low (45%), implying low monomer conversion during polymerization, which is resulted from insufficient amount of BPO in the pellets. With more addition of St (10–25%), the monomer efficiency is 80–89%, revealing high diffusion efficiency of both St and BPO. Since BPO diffuses into the pellets along the diffusion path of St, the diffusion efficiency of BPO depends on the amount of St in the pellets. When the amount of St in the pellets is small, the diffusion path of BPO is not well established and thus the diffusion efficiency of BPO is low, and that is the case of 5% St addition. By contrast, sufficient St in the pellets can ensure high diffusion efficiency of BPO, such as in the cases of 10–25% St addition.

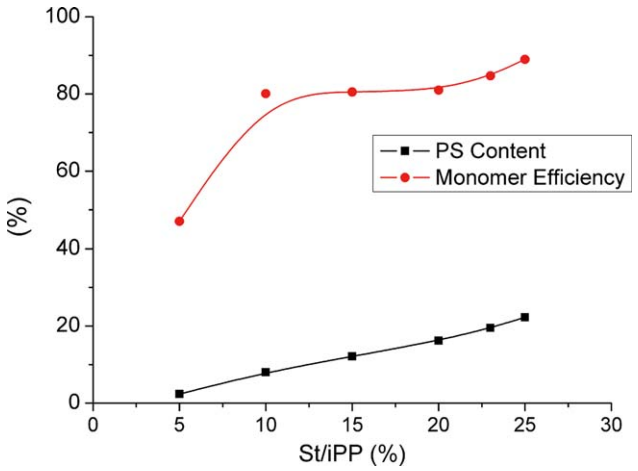

Figure 2. PS contents and monomer efficiencies at different amounts of St. (iPP is fixed at 600 g). [Color figure can be viewed in the online issue, which is available at wileyonlinelibrary.com.]

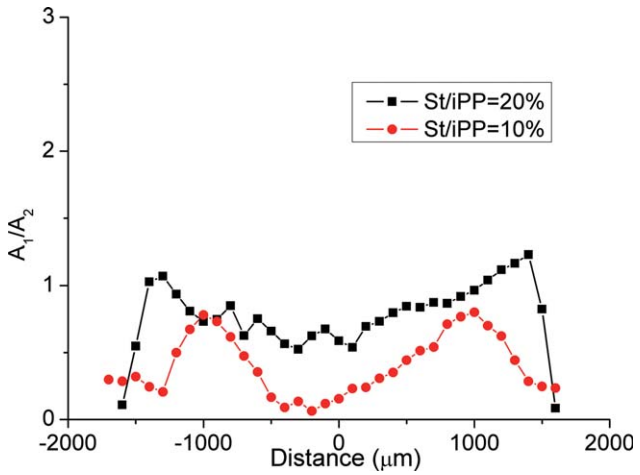

Figure 3. Micro-FTIR profiles of iPP/PS pellets synthesized with 10% St and 20% St along the diameter direction (distance 0 is the center of the pellets). [Color figure can be viewed in the online issue, which is available at wileyonlinelibrary.com.]

Distribution of PS and Morphology of the Blend Pellets

The diametrical distribution of PS in the PP/PS blend pellets synthesized with 10% St and 20% St were investigated by Micro-FTIR, and the spectra are shown in Figure 3. Distance 0 is the center of the pellets. The distribution of PS along the diameter direction is almost homogeneous for the sample prepared with 20% St, while it shows two maxima at about 700 μm to the edge for the sample prepared with 10% St. This suggests that the distributions of both St and BPO in the pellets at the beginning of the initiation are homogeneous when the amounts of St and BPO are large, and inhomogeneous distribution of BPO may happen when the amounts of St and BPO are small. It could be speculated that the position at 700 μm to the edge contains more BPO than other places at the beginning of the initiation, and upon polymerization the St at other places migrates to that position (and then polymerizes there) through polymerization-induced diffusion of St, resulting in the formation of more PS at that position than at other places. The driving force for polymerization-induced diffusion of St toward the early-polymerized position is the increased PS content and decreased monomer concentration in the amorphous PP phase as polymerization proceeds, both needing more monomer to establish new swelling equilibrium.

The morphology of a typical blend pellet, the one synthesized with 20% St, was investigated by Field Emission Scanning Electron Microscopy (FESEM) after etching the amorphous PP portions for a better observation. The FESEM micrographs of three positions in the cross-section fractured across the center of the pellet (center, mid-depth from the surface to the center, and 300 μm to the edge) are shown in Figure 4. Most of the PS particles at the center and mid-depth are around 100 nm, although few slightly bigger particles are also present. At 300 μm to the edge, the average particle size is bigger (101 nm) than those of the two other places just mentioned (78 and 86 nm), some bigger-sized PS particles are observed but their sizes are less than 300 nm. The PS particle sizes in this blend pellet are considerably less than those reported previously[10] for two reasons. Firstly, this blend was synthesized in two steps in which the

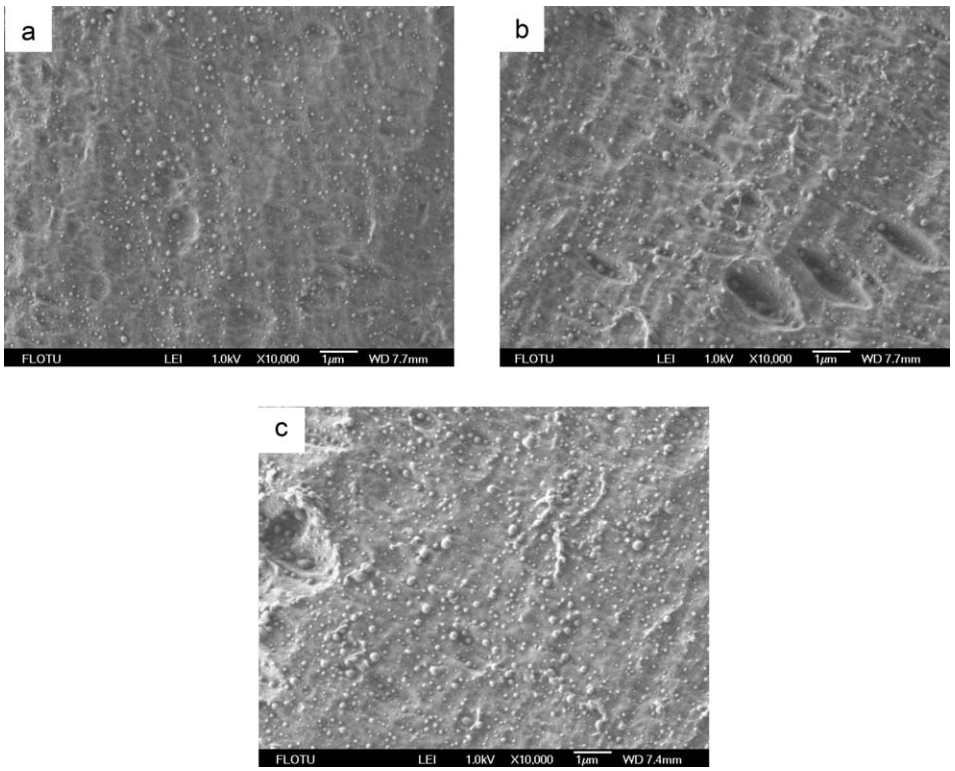

Figure 4. FESEM images of the cross-section of a typical iPP/PS blend pellet synthesized with 20% St and 600 g PP after etching: (a) at the center; (b) at mid-depth from the surface to the center; and (c) near the surface.

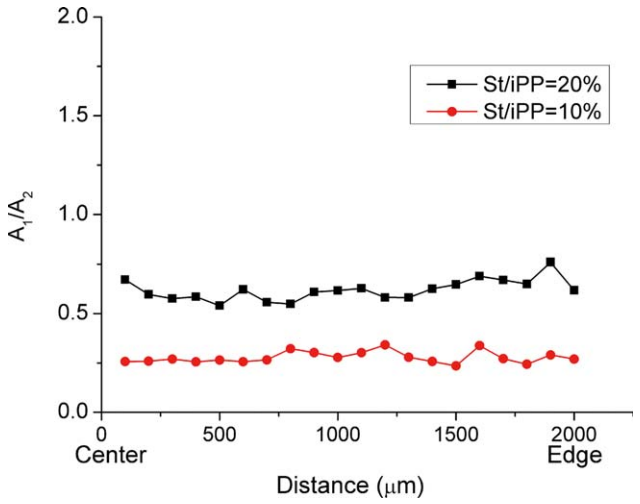

Figure 5. Micro-FTIR profiles of injection-molded bars of iPP/PS pellets synthesized with 10% and 20% St, and 600 g PP pellets. [Color figure can be viewed in the online issue, which is available at wileyonlinelibrary.com.]

excess St that is not diffused into the pellet in the diffusion step is removed by filtration, and there is almost no occurrence of further diffusion of St from outside to inside the pellets during polymerization. Secondly, less St was used in the synthesis of this blend pellet than in the previous work (20% vs. 30%). In some pellets, there is a hole at the center of the pellets, which is formed during granulation of PP pellets, and no PS was found in the hole.

Distribution of PS and Morphology of the Injection-Molded Bars

The injection-molded bars produced with the blend pellets synthesized from 10% St and 20% St were cut through the cross-section direction and Micro-FTIR was performed along the thickness direction. As shown in Figure 5, the PS distribution from the edge to the center is almost homogeneous for both samples no matter whether the PS distribution in the blend pellets is homogeneous. This confirms that the fed pellets are homogenized to a certain degree even at low shear rate of injection molding.

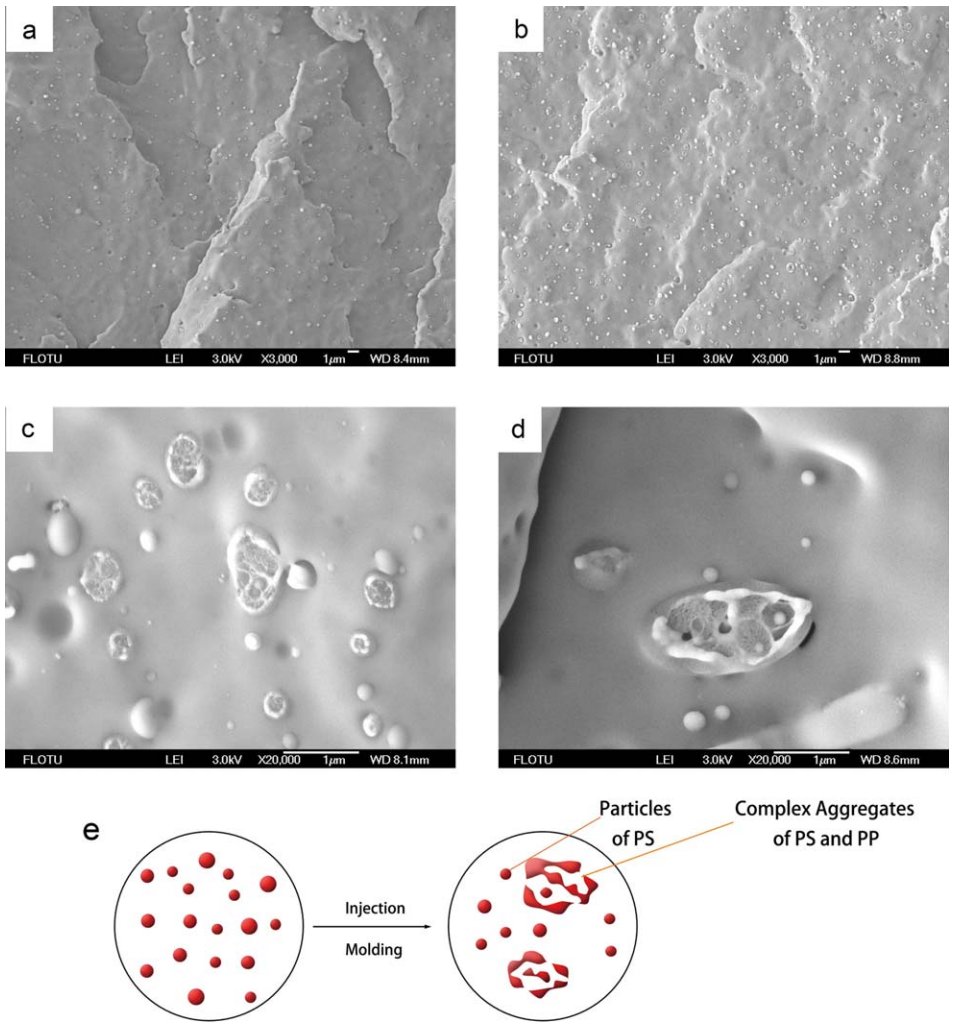

Figure 6. FESEM images of the cross-sections of injection-molded bars of iPP/PS pellets synthesized with (a,c) St/iPP = 10 wt % and (b,d) St/iPP = 20 wt % at two different magnifications: (a,b) ×3000 and (c,d) ×20,000, and (e) Schematic illustration of phase morphology evolution during injection molding. [Color figure can be viewed in the online issue, which is available at wileyonlinelibrary.com.]

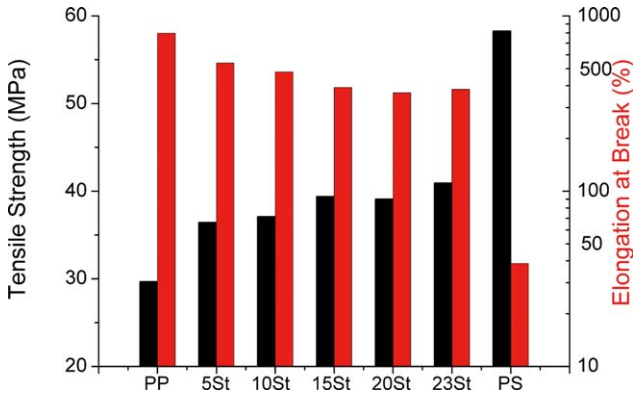

Figure 7. Mechanical properties of the injection-molded bars of the blend pellets synthesized with 600 g PP pellets and different amounts of St, neat PP and neat PS (XSt means St/iPP ratio is X%). [Color figure can be viewed in the online issue, which is available at wileyonlinelibrary.com.]

The morphology of injection-molded bars for the two samples mentioned above was investigated by FESEM. Figure 6 shows the micrographs of the cryo-fractured cross-sections at two different magnifications. At low magnification (×3000), particles of sizes higher than those in the corresponding pellets are observed, mainly in nano and submicron sizes, and only few particles approach 1 μm. This indicates occurrence of slight coalescence during injection molding. Comparing the two samples [Figure 6(a,b)], the main difference is the particle number, much more in the sample with higher PS content, and there is no significant difference in particle size. The boundary between the particles and the matrix is quite ambiguous in both samples, indicating good interfacial adhesion, which is attributed to the existence of PS grafting on PP chains (i.e., PS-*g*-PP) formed during polymerization. At high magnification [×20,000, Figure 6(c,d)], two types of particles are observed, one is spherical and the other is irregular in shape and generally bigger in size. The spherical particles are supposed to be the primary particles retained from the pellets. As illustrated in Figure 6(e), the bigger and irregular particles are not pure coalesced PS, but complex aggregates of spherical PS particles, elongated, arc-, and T-shaped PS particles and PP. The reason for the formation of this type of complex structure may be attributed to the existence of PS grafting on PP chains, coupled with low shear rate of injection molding. The percentage of grafting is 1.9% for the blend pellets synthesized from 20% St. During injection molding, coalescence of PS particles is inhibited to a certain degree by the PP chains grafted by PS.

Mechanical Properties of the Injection-Molded Bars

Uniaxial tensile testing was used to evaluate the mechanical properties of the injection-molded bars. As shown in Figure 7, all the PP/PS blends synthesized with 5–23% St (corresponding to PS contents of 3–18%) show considerably improved yield strength compared to neat PP. Even with a very small PS content (3%), the yield strength has a 20% increase. When the PS content increases to 18%, the yield strength increases to 36 from 29 MPa (neat PP), an improvement of 27%. The improved yield strength can be explained by the good interfacial adhesion between the dispersed particles and the matrix phase, mentioned earlier in the section of morphology. Because both the PS particles and the complex aggregates are stiffer than PP, and also because the interfacial adhesion is good enough to support load transfer from the matrix to particles, a reinforcing effect is achieved.

The elongations at break of all the PP/PS blends are over 300%, revealing the maintenance of good ductility of PP despite of the incorporation of stiff PS. To explain this phenomenon, the necking region of the elongated tensile bar (Sample with 20% St) after tensile test was fractured perpendicularly to the stretching direction, and the resulted longitudinal cross-section was observed by FESEM. As shown in Figure 8, the particles are localized among the aligned microfibrils and do not act as stress concentrators because of their small size and good interfacial adhesion with the matrix, and therefore all the PP/PS blends exhibit good ductility although PS is brittle.

In contrast to the microphase-separated PP/PS blends discussed above, PP/PS blends prepared using conventional melt mixing show indeed macrophase-separated structure (Figure 9). Therefore, the PP/PS quasi-nanoblend pellets prepared by the method of diffusion and subsequent polymerization are useful and

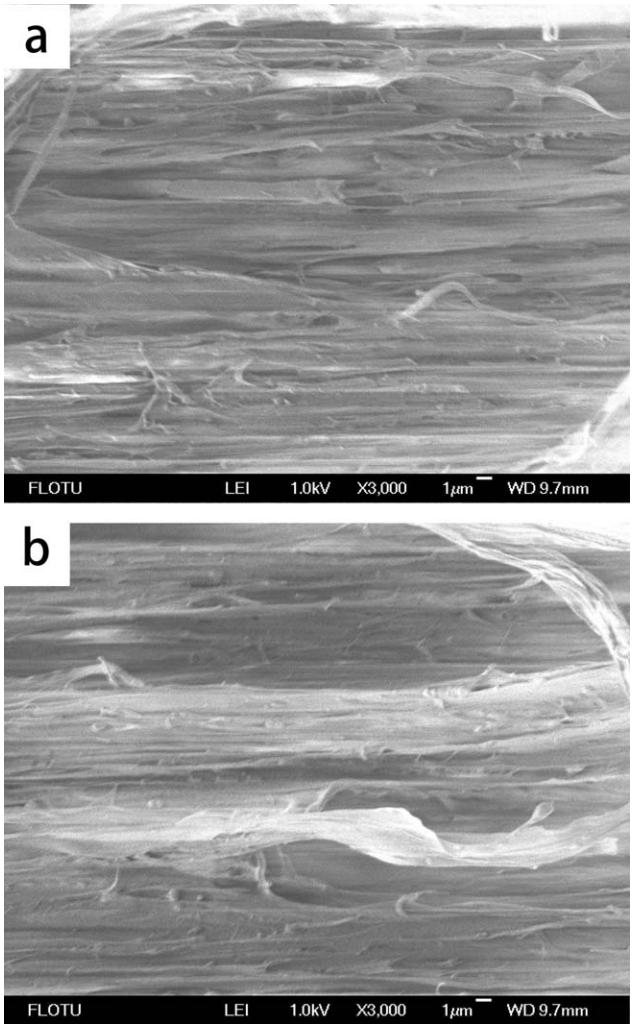

Figure 8. FESEM images of the longitudinal cross-section of the elongated tensile bar (Sample with 20% St) fractured perpendicularly to the stretching direction.

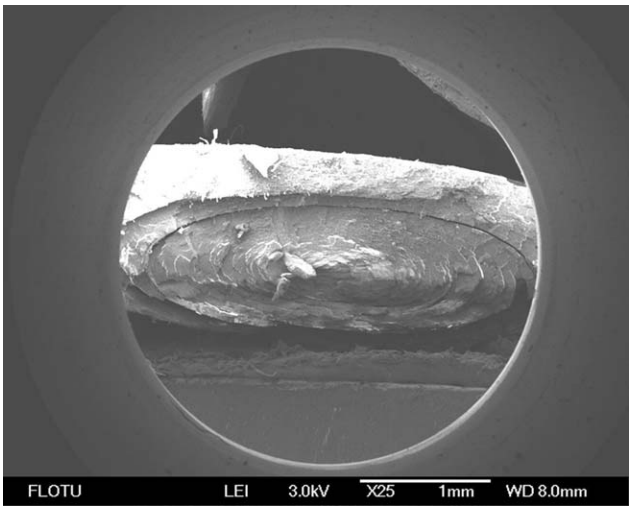

Figure 9. FESEM image of the cross-section of PP/PS blends prepared using conventional melt mixing.

unique stock for further manufacturing processes to produce plastic products.

CONCLUSIONS

Useful PP/PS injection-molded bars can be obtained by injection molding of the PP/PS quasi-nanoblend pellets synthesized by the method of diffusion and subsequent polymerization of St in iPP pellets. The PS distribution along the thickness direction of the injection-molded bars is almost homogeneous for all the blends no matter whether the PS distribution in the blend pellets is homogeneous. The PP/PS injection-molded bars show microphase-separated structure rather than macrophase-separated structure observed from conventional melt mixing. There are two types of particles in PP/PS bars: small spherical and bigger irregular-shaped complex aggregates. The former are supposed to be the primary particles retained from the pellets. The latter are not pure coalesced PS, but complex aggregates composed of spherical PS particles, elongated, arc-, and T-shaped PS particles and PP. They are mainly in nano and submicron sizes, and only few particles approach 1 μm. They have good interfacial adhesion with the matrix as indicated by the ambiguous boundary. This type of morphology results in good reinforcing effect without significantly loosing ductility. The yield strength increases from 29 MPa (neat PP) to 36 MPa with a PS content of 18%, and the elongation at break is still over 300%. This work proves that the diffusion and subsequent polymerization of styrene in iPP pellets is a valuable method to synthesize PP/PS blend pellets in preparation for low-shear manufacturing processes such as injection molding.

ACKNOWLEDGMENTS

The authors gratefully acknowledge the financial support from the National Natural Science Foundation of China (No. 51173095).

REFERENCES

1. Hu, G. H.; Cartier, H.; Plummer, C. *Macromolecules* **1999**, *32*, 4713.
2. Ibuki, J.; Charoensirisomboon, P.; Chiba, T.; Ougizawa, T.; Inoue, T.; Weber, M.; Koch, E. *Polymer* **1999**, *40*, 647.
3. Liu, Z. M.; Dong, Z. X.; Han, B. X.; Wang, J. Q.; He, J.; Yang, G. Y. *Chem. Mater.* **2002**, *14*, 4619.
4. Chan, S. H.; Lin, Y. Y.; Ting, C. *Macromolecules* **2003**, *36*, 8910.
5. Ji, Y. L.; Li, W. G.; Ma, J. H.; Liang, B. R. *Macromol. Rapid Commun.* **2005**, *26*, 116.
6. Shimizu, H.; Li, Y. J.; Kaito, A.; Sano, H. *Macromolecules* **2005**, *38*, 7880.
7. Tao, Y.; Kim, J.; Torkelson, J. M. *Polymer* **2006**, *47*, 6773.
8. Li, Y. J.; Wakura, Y.; Zhao, L.; Shimizu, H. *Macromolecules* **2008**, *41*, 3120.
9. Walther, A.; Matussek, K.; Muller, A. H. E. *ACS Nano* **2008**, *2*, 1167.
10. Yao, X. R.; Yu, J.; Guo, Z. X. *Polymer* **2011**, *52*, 667.
11. Zhu, R.; Hoshi, T.; Chishima, Y.; Muroga, Y.; Hagiwara, T.; Yano, S.; Sawaguchi, T. *Macromolecules* **2011**, *44*, 6103.
12. Yao, X. R.; Wang, L.; Guo, Z. X.; Yu, J. *J. Appl. Polym. Sci.* **2013**, *127*, 1092.
13. Costa, L. C.; Neto, A. T.; Hage, E. *Express Polym. Lett* **2014**, *8*, 164.
14. Kausar, A.; Zulfiqar, S.; Sarwar, M. I. *J. Appl. Polym. Sci.* **2014**, *131*, DOI: 10.1002/app.39954.
15. Kausar, A.; Zulfiqar, S.; Sarwar, M. I. *Polym. Adv. Technol* **2014**, *25*, 196.
16. Qiu, H. Y.; Chen, F.; Guo, Z. X.; Yu, J. *Chin. J. Polym. Sci.* **2015**, *33*, 1380.
17. Naylor, A.; Howdle, S. M. *J. Mater. Chem.* **2005**, *15*, 5037.
18. Liu, Z. M.; Wang, J. Q.; Dai, X. H.; Han, B. X.; Dong, Z. X.; Yang, G. Y.; Zhang, X. L.; Xu, J. *J. Mater. Chem.* **2002**, *12*, 2688.
19. Li, D.; Liu, Z. M.; Han, B. X.; Song, L. P.; Yang, G. Y.; Jiang, T. *Polymer* **2002**, *43*, 5363.
20. Li, D.; Han, B. X. *Macromolecules* **2000**, *33*, 4555.
21. Li, D.; Han, B. X. *Ind. Eng. Chem. Res.* **2000**, *39*, 4506.